Title

Safe Reconnection Time for Large-Scale Data Center Loads: An Analytical Framework for Transient Stability Assessment

Journal

Proceedings of the PowerUp Conference, 1(1)

Authors

Alkhudaydi, Ahmed Mesfer
Cui, Bai

Publication Date

2026-09-09

DOI

None/powerup_proceedings.69097

Safe Reconnection Time for Large-Scale Data Center Loads: An Analytical Framework for Transient Stability Assessment

Ahmed Alkhudaydi, Bai Cui

Iowa State University

Suggested Citation

A. Alkhudaydi and B. Cui, "Safe Reconnection Time for Large-Scale Data Center Loads: An Analytical Framework for Transient Stability Assessment," in *Proceedings of the PowerUp Conference*, 2026.

BibTeX Entry

```
@inproceedings{cui2026safereconnection,
  author = {Alkhudaydi, Ahmed and Cui, Bai},
  title = {Safe Reconnection Time for Large-Scale Data Center Loads: An Analytical
      Framework for Transient Stability Assessment},
  booktitle = {Proceedings of the PowerUp Conference},
  year = {2026},
}
```

Safe Reconnection Time for Large-Scale Data Center Loads: An Analytical Framework for Transient Stability Assessment

Ahmed Mesfer Alkhudaydi and Bai Cui

***Abstract*—The rapid growth of large, power electronics-rich data center loads (DCLs) is creating new operational challenges for bulk power systems. A key risk arises when a DCLs uninterruptible power supply (UPS) disconnects the facility during voltage/frequency disturbances and then reconnects it while the bulk grid is still dynamically settling to a new equilibrium point. Poorly timed reconnection can amplify electromechanical oscillations, deepen frequency deviations, and lead to repeated connect-disconnect *flapping*. In this paper, we develop an analytical framework to characterize the *safe reconnection time* for large DCL after a disturbance-induced disconnection that avoids flapping. Using a model in the spirit of the classical single-machine infinite-bus system, we capture (i) swing dynamics during the disconnection interval and (ii) voltage-angle coupling at the load bus, which determines the electrical power step at reconnection under constant-power load assumptions. Using energy function method, we characterize the critical safe reconnection time such that for any reconnection time after the critical safe reconnection time, the post-reconnection trajectory is guaranteed to remain within operational limits (frequency/angle/voltage) and converge to the post-reconnection equilibrium, thereby preventing flapping. Time-domain simulations validate the effectiveness of the proposed analytical approach. The results provide a simple, physics-informed criterion that can be used to bound reconnection windows for large DCL facilities and inform UPS reconnection logic.**

***Index Terms*—Data centers, reconnection timing, transient stability, voltage-angle coupling.**

I. Introduction

Data center loads (DCLs) are becoming one of the fastest-growing classes of electricity demand, driven by cloud services and AI workloads. Recent international assessments highlight both the current scale and the potential for significant growth in DCL electricity consumption over this decade [1], [2]. In 2022, global DCL power consumption reached approximately 460 TWh, representing nearly 2% of worldwide electricity demand, with projections indicating a potential doubling by 2030 [2]. This rapid expansion poses significant challenges for transmission system operators (TSOs), particularly in island power systems and regions with high renewable energy penetration which have limited inertia or constrained interconnection, where large step changes in demand can translate into material voltage and frequency excursions [3], [4].

Unlike many traditional industrial loads, DCLs exhibit unique operational characteristics that complicate power system stability analysis. Modern DCLs are equipped with uninterruptible power supply (UPS) systems that provide fault ride-through capability but also introduce complex disconnection and reconnection logic based on voltage and frequency thresholds [5]–[8]. During grid disturbances, these protection systems can abruptly disconnect hundreds of megawatts of load, causing substantial frequency excursions that trigger cascading stability concerns [9]. From a transmission system perspective, the disturbance response is not limited to the initial disconnection. The reconnection moment can be equally (or more) consequential: if reconnection occurs while generator rotor dynamics are still settling, the resulting load step may (i) deepen the frequency nadir, (ii) increase rate of change of frequency (RoCoF), and/or (iii) excite electromechanical oscillations that push voltage or frequency back across the UPS trip thresholds, which is a phenomenon known as *flapping* where the DCL repeatedly connects and disconnects, further degrading system stability [10].

Real-world incidents underscore the severity of this issue. In the all-island Irish transmission system, a fault in 2023 resulted in a 204 MW instantaneous drop in DCL demand, producing a RoCoF of 0.12 Hz/s and a frequency nadir of 49.78 Hz [11]. Ireland's position as an island system with limited interconnection capacity , together with rapidly growing DCL penetration, makes it particularly vulnerable to such events. DCL currently represents approximately 11% of peak demand in Ireland, with projections reaching 23% by 2030 [12]. Similar challenges have been documented in Nordic systems and are emerging in continental Europe as DCL concentration increases in specific geographic regions [13].

Recent work in [10] developed a comprehensive DCL model incorporating UPS dynamics, cooling system induction motors, and time-varying computational loads, which provides valuable insights into DCLs behavior during faults. However, their work did not address the optimization of reconnection timing to prevent post-fault instability. The determination of optimal reconnection time presents a challenging nonlinear optimization problem. The rotor angle and speed of synchronous generators evolve according to swing dynamics during the disconnection period, while the reconnection instant must satisfy both pre-connection constraints (adequate frequency and voltage recovery) and post-connection constraints (avoiding excessive oscillations that trigger re-disconnection). Furthermore, the electrical power demanded by the DCL exhibits a strong nonlinear dependence on the generator rotor angle through voltage–angle coupling, which makes the solution more challenging [14].

To connect DCL dynamics with actionable operational decisions, we propose an analytical framework for safe reconnection time characterization following UPS-triggered disconnection. Our contributions are threefold: first, we develop a three-bus single-machine infinite-bus (SMIB) extension that retains voltage–angle coupling at the load bus while isolating the effect of reconnection timing; second, we develop a hybrid system representation of DCL disconnection/reconnection dynamics through explicit switching logic; third, we formulate

A. M. Alkhudaydi and B. Cui are with the Department of Electrical and Computer Engineering, Iowa State University, Ames, IA 50011 USA. Emails: {ahmed92, baicui}@iastate.edu

a series of optimization problems for determining the earliest safe reconnection time. The overall framework facilitates rapid computation of safe reconnection windows suitable for real-time operations.

The remainder of this paper is organized as follows. Section II presents the system model, including the configuration of three-bus system, the swing equation, and the characteristics of the DCL. Section III formalizes the problem of characterizing the safe reconnection time of DCL post-disturbance. Section IV develops an energy function-based certification method to compute the earliest safe reconnection time. Section V presents time-domain simulations of the proposed approach. Finally, Section VI concludes the paper.

II. System Modeling

A. A Simplified Three-Bus Power System Configuration

We consider a simplified three-bus power system model, shown in Fig. 1, which extends the classical single-machine infinite-bus (SMIB) framework by explicitly introducing a dedicated DCL bus while preserving analytical tractability. Bus 1 represents a synchronous generator described by the second-order swing dynamics with an internal voltage $e\angle\delta$, where δ is the rotor angle referenced to the infinite bus. Bus 2 is the DCL bus, characterized by a constant power demand $(p_{\mathrm{DCL}}, q_{\mathrm{DCL}})$ and bus voltage $v\angle\phi$. Bus 3 is modeled as an infinite bus with fixed voltage $1\angle 0°$, representing the external grid. The generator is connected to bus 2 through the transient reactance x_d', which is suitable for stability at the first-swing and analysis of short-term disturbances [15]. The transmission line connecting bus 2 and bus 3 has a reactance x_l that varies according to the conditions of the system where x_l^{pre} in normal operation, x_l^{f} during fault, and x_l^{post} after a fault is cleared.

Under steady-state conditions, bus 1, bus 2, and bus 3 are modeled as PV bus, PQ bus, and reference bus, respectively. For simplicity, we assume that the voltage magnitude at bus 1, the back emf of the synchronous generator, is constant, even during transients. This assumption is standard in classical first-swing transient stability analysis [9], [16], where the generator internal emf behind transient reactance is treated as approximately constant during the electromechanical swing. This approximation is most appropriate when the study focuses on the first-swing response, the generator remains within its reactive power capability, and the AVR or excitation limiters do not dominate the voltage response. Including explicit AVR dynamics or fast reactive power support would change the post-reconnection voltage trajectory at bus 2 and therefore affect the DCL voltage bound constraints. A detailed treatment of these effects is beyond the scope of this work and is left for future study.

B. Simulation Framework

The dynamic behavior of the system is analyzed through four distinct stages: pre-fault steady state, fault-on dynamics, post-fault islanded operation, and reconnection. Each stage captures specific aspects of the interaction between the generator and the DCL during disturbances.

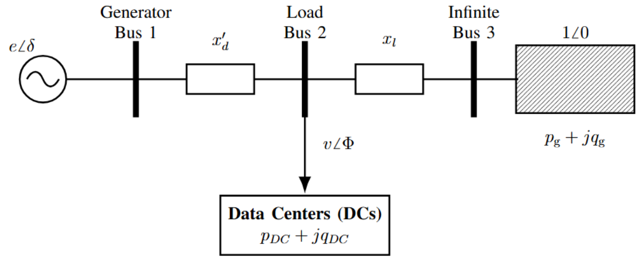

Fig. 1. A simplified three-bus system

*1) **Pre-fault State** $(t < 0)$:* The generator supplies the DCL and the infinite bus. The system can be characterized by the steady state model as follows:

$$-p_{\mathrm{DCL}} = \frac{ev^{\mathrm{ss}}\sin(\phi^{\mathrm{ss}} - \delta^{\mathrm{ss}})}{x_d'} + \frac{v^{\mathrm{ss}}\sin\phi^{\mathrm{ss}}}{x_l^{\mathrm{pre}}}, \tag{1a}$$

$$-q_{\mathrm{DCL}} = \frac{(v^{\mathrm{ss}})^2 - ev^{\mathrm{ss}}\cos(\phi^{\mathrm{ss}} - \delta^{\mathrm{ss}})}{x_d'} + \frac{(v^{\mathrm{ss}})^2 - v^{\mathrm{ss}}\cos\phi^{\mathrm{ss}}}{x_l^{\mathrm{pre}}}, \tag{1b}$$

$$p_g = \frac{ev^{\mathrm{ss}}\sin(\delta^{\mathrm{ss}} - \phi^{\mathrm{ss}})}{x_d'}. \tag{1c}$$

Here, $p_{\mathrm{DCL}}, q_{\mathrm{DCL}}, p_g, x_d', x_l^{\mathrm{pre}}$, and e are given parameters, while $v^{\mathrm{ss}}, \phi^{\mathrm{ss}}$, and δ^{ss} are unknown steady state variables.

Solving for $\sin(\delta^{\mathrm{ss}} - \phi^{\mathrm{ss}})$ in (1c) and $\sin\phi^{\mathrm{ss}}$ in (1a) leads to the following expressions:

$$\sin(\delta^{\mathrm{ss}} - \phi^{\mathrm{ss}}) = \frac{p_g x_d'}{ev^{\mathrm{ss}}}, \tag{2a}$$

$$\sin\phi^{\mathrm{ss}} = \frac{(p_g - p_{\mathrm{DCL}})\, x_l^{\mathrm{pre}}}{v^{\mathrm{ss}}}. \tag{2b}$$

We can then replace $\cos(\delta^{\mathrm{ss}} - \phi^{\mathrm{ss}})$ and $\cos\phi^{\mathrm{ss}}$ in (1b) by solving for them in (2), which leads to:

$$\begin{aligned} -q_{\mathrm{DCL}} = {} & \left(\frac{1}{x_d'} + \frac{1}{x_l^{\mathrm{pre}}}\right)(v^{\mathrm{ss}})^2 - \frac{\sqrt{e^2(v^{\mathrm{ss}})^2 - p_g^2 x_d'^2}}{x_d'} \\ & - \frac{\sqrt{(v^{\mathrm{ss}})^2 - (p_g - p_{\mathrm{DCL}})^2 (x_l^{\mathrm{pre}})^2}}{x_l^{\mathrm{pre}}}, \end{aligned} \tag{3}$$

where we assume $\delta^{\mathrm{ss}} - \phi, \phi \in [-\pi/2, \pi/2]$.

Equation (3) is a quartic equation in v^2 that is cumbersome to solve directly. A simpler solution approach is to cast it in fixed-point form and apply fixed-point iteration:

$$\begin{aligned} v^{\mathrm{ss}} = {} & \frac{x_l^{\mathrm{pre}}}{x_d' + x_l^{\mathrm{pre}}}\sqrt{e^2 - \frac{p_g^2 x_d'^2}{(v^{\mathrm{ss}})^2}} \\ & + \frac{x_d'}{x_d' + x_l^{\mathrm{pre}}}\sqrt{1 - \frac{(p_g - p_{\mathrm{DCL}})^2 (x_l^{\mathrm{pre}})^2}{(v^{\mathrm{ss}})^2}} \\ & - \frac{x_d' x_l^{\mathrm{pre}}}{x_d' + x_l^{\mathrm{pre}}}\frac{q_{\mathrm{DCL}}}{v^{\mathrm{ss}}}. \end{aligned} \tag{4}$$

After obtaining the steady-state voltage v^{ss}, the phase angles δ^{ss} and ϕ^{ss} can be obtained from (2).

Remark 1. *The fixed-point iteration* (4) *is well-defined when the square root arguments remain nonnegative; convergence* *is expected when the operating point is sufficiently far from voltage collapse so that the corresponding map remains locally contractive.*

*2) **Fault On and DCL Disconnection State*** ($t = 0 = t_{\rm dis}$)*:* A fault is represented by increasing the line impedance jx_l between bus 2 and bus 3 from $x_l^{\rm pre}$ to $x_l^{\rm f}$. The network reduces to an equivalent two-bus system:

$$\begin{aligned}\tilde{e}_{\rm eq}^{\rm f}(\delta) &= \frac{e\angle\delta/x_d'}{1/x_d' + 1/x_l^{\rm f}} + \frac{1/x_l^{\rm f}}{1/x_d' + 1/x_l^{\rm f}} \\ &= \frac{(x_l^{\rm f} e\cos\delta + x_d') + jx_l^{\rm f} e\sin\delta}{x_d' + x_l^{\rm f}},\end{aligned} \tag{5a}$$

$$x_{\rm eq}^{\rm f} = \frac{1}{1/x_d' + 1/x_l^{\rm f}} = \frac{x_d' x_l^{\rm f}}{x_d' + x_l^{\rm f}}. \tag{5b}$$

Under constant PQ loading, the voltage magnitude at bus 2 satisfies

$$v^2 = \frac{|\tilde{e}_{\rm eq}^{\rm f}|^2 + 2x_{\rm eq}^{\rm f} q_{\rm DCL} + \Delta^{\rm f}}{2}. \tag{6}$$

where the discriminant $\Delta^{\rm f}$ is

$$\Delta^{\rm f} = \left(|\tilde{e}_{\rm eq}^{\rm f}|^2 + 2x_{\rm eq}^{\rm f} q_{\rm DCL}\right)^2 - 4\left(x_{\rm eq}^{\rm f}\right)^2\left(p_{\rm DCL}^2 + q_{\rm DCL}^2\right).$$

The voltage angle is computed as

$$\phi^{\rm f}(\delta) = \delta + \angle\left(v^2 + 2x_{\rm eq}^{\rm f} q_{\rm DCL} - jx_{\rm eq}^{\rm f} p_{\rm DCL}\right). \tag{7}$$

This voltage-angle coupling creates path dependent stability characteristics. As the rotor swings during the disconnection period, the voltage that would appear at bus 2 upon reconnection varies, directly affecting the magnitude of the reconnection transient.

*3) **DCL Disconnection/Fault Clearing to Reconnection State*** ($0 < t < t_{\rm re}$)*:* Assuming DCL disconnection occurs at $t = 0$ and the fault is cleared immediately to the post-fault value $x_l^{\rm post}$. During this waiting period, the generator operates without the DCL, settling toward a no-load equilibrium angle $\delta_{\rm eq}^{\text{no-load}}$ defined by the power balance:

$$p_g = \frac{e\sin(\delta_{\rm eq}^{\text{no-load}})}{x_d' + x_l^{\rm post}}, \tag{8a}$$

$$\delta_{\rm eq}^{\text{no-load}} = \arcsin\left(\frac{p_g\,(x_d' + x_l^{\rm post})}{e}\right). \tag{8b}$$

The system dynamics are therefore governed by the swing equations

$$\dot{\delta} = \omega, \tag{9a}$$

$$M\dot{\omega} = p_g - \frac{e}{x_d' + x_l^{\rm post}}\sin\delta - D\omega, \tag{9b}$$

where M is the generator inertia constant and D is the damping coefficient.

*4) **Reconnection State*** ($t \geq t_{\rm re}$)*:* After reconnection, the post-fault equivalent system parameters are

$$\begin{aligned}\tilde{e}_{\rm eq}^{\rm post}(\delta) &= \frac{e\angle\delta/x_d'}{1/x_d' + 1/x_l^{\rm post}} + \frac{1/x_l^{\rm post}}{1/x_d' + 1/x_l^{\rm post}} \\ &= \frac{(x_l^{\rm post} e\cos\delta + x_d') + jx_l^{\rm post} e\sin\delta}{x_d' + x_l^{\rm post}},\end{aligned} \tag{10a}$$

$$x_{\rm eq}^{\rm post} = \frac{1}{1/x_d' + 1/x_l^{\rm post}} = \frac{x_d' x_l^{\rm post}}{x_d' + x_l^{\rm post}}. \tag{10b}$$

The bus 2 voltage magnitude and phase angle are

$$v^{\rm post}(\delta) = \left(\frac{|\tilde{e}_{\rm eq}^{\rm post}(\delta)|^2 + 2x_{\rm eq}^{\rm post} q_{\rm DCL} + \sqrt{\Delta^{\rm post}}}{2}\right)^{1/2}, \tag{11a}$$

$$\phi^{\rm post}(\delta) = \delta + \angle\left(v^{\rm post}(\delta) + x_{\rm eq}^{\rm post} q_{\rm DCL} - jx_{\rm eq}^{\rm post} p_{\rm DCL}\right) \tag{11b}$$

where the discriminant is given via

$$\Delta^{\rm post} = \left(|\tilde{e}_{\rm eq}^{\rm post}(\delta)|^2 + 2x_{\rm eq}^{\rm post} q_{\rm DCL}\right)^2 - 4\left(x_{\rm eq}^{\rm post}\right)^2\left(p_{\rm DCL}^2 + q_{\rm DCL}^2\right).$$

The post-reconnection system dynamics are governed by:

$$\dot{\delta} = \omega, \tag{12a}$$

$$M\dot{\omega} = p_g - \frac{ev^{\rm post}(\delta)}{x_d'}\sin\left(\delta - \phi^{\rm post}(\delta)\right) - D\omega. \tag{12b}$$

The reconnection dynamic model above captures the flapping phenomenon that can occur if the reconnection timing is not properly coordinated with the system's dynamic state. The interdependence between δ, $v^{\rm post}(\delta)$, and $\phi^{\rm post}(\delta)$ in (11a)-(11b) indicates the coupling between generator dynamics and load voltage recovery during the reconnection process.

III. Problem Formulation

In this section, we develop a direct method to determine the earliest reconnection time $t_{\rm re}^{\star}$ for the DCL, such that for any reconnection time $t \geq t_{\rm re}^{\star}$, the post-reconnection trajectory is stable and remains within operational protection limits to prevent repeated disconnections (flapping).

Let the generator swing state be $x(t) := [\delta(t), \omega(t)]^{\top}$ and denote the post-reconnection (DCL-connected) stable equilibrium by $(\delta_{\rm eq}^{\rm load}, 0)$. Here $t_{\rm re}^{\star}$ acts as a switching time where it determines the state at reconnection $x(t_{\rm re})$, which is the initial condition for the post-reconnection dynamics.

A. Hybrid Evolution and Waiting Trajectory

The reconnection time $t_{\rm re}^{\star} > 0$ determines the switching instant between pre- and post-reconnection dynamics.

During the waiting interval $0 \leq t < t_{\rm re}$, the state $x(t)$ evolves under the pre-reconnection swing dynamics (DCL-disconnected), cf. (9). At $t = t_{\rm re}^{\star}$, the DCL is reconnected and the post-reconnection dynamics apply, cf. (12). This mirrors the role of fault clearing time in classical transient stability analysis where changing $t_{\rm re}^{\star}$ changes the switching state $x(t_{\rm re}^{\star})$ and thus the subsequent trajectory.

B. Safe Initial Condition Set for Reconnection

We adopt a cascaded formulation where a set of post-reconnection initial conditions, which are guaranteed to be safe, is characterized. Then, the reconnection time $t_{\rm re}^{\star}$ is selected such that the waiting trajectory enters this set.

1) Protection band in the (δ, ω) plane: Operational protection limits on rotor angle and frequency deviations are defined with respect to the post-reconnection equilibrium $(\delta_{\text{eq}}^{\text{load}}, 0)$ as

$$|\delta - \delta_{\text{eq}}^{\text{load}}| \le \delta_{\max}, \quad |\Delta\omega| \le \omega_{\max}. \tag{13}$$

These bounds represent physical constraints, where $\delta_{\max}$ limits angular separation to prevent loss of synchronism, while $\omega_{\max}$ enforces frequency protection relay settings, typically ± 0.5 to ± 1.0 Hz from nominal frequency, corresponding to $\omega_{\max} \approx \pi$ to 2π rad/s for 50/60 Hz systems [17], [18].

2) Voltage bounds: In the reduced order model, the voltage magnitude at bus 2 after reconnection is determined algebraically from the post-reconnection network reduction and the constant power DCL model, which is given as $v^{\text{post}}(\delta)$ in (11). This voltage must satisfy operational bounds as

$$v_{\min} \le v^{\text{post}}(\delta) \le v_{\max}. \tag{14}$$

Although $v^{\text{post}}(\delta)$ depends only on δ as shown (11), the voltage constraint must be explicitly enforced, as the nonlinear voltage-angle coupling does not guaranty the satisfaction of (14) solely from the rotor angle limits. Therefore, we define the admissible reconnection set as the set of post-reconnection initial conditions that satisfy both the protection band and the voltage admissibility conditions as

$$\mathcal{S}_{\text{adm}} := \left\{ (\delta, \Delta\omega) \in \mathbb{R}^2 \;\middle|\; \begin{array}{c} |\delta - \delta_{\text{eq}}^{\text{load}}| \le \delta_{\max}, \\ |\Delta\omega| \le \omega_{\max}, \\ v_{\min} \le v^{\text{post}}(\delta) \le v_{\max} \end{array} \right\}. \tag{15}$$

Specifically, the *flapping* occurs when the post-reconnection trajectory violates the protection limits in (13)–(14), which re-triggers the UPS disconnection condition and initiates a repeated connect-disconnect cycle.

It is worth noting that the proposed method treats any instantaneous violation of the protection thresholds as a disconnection event. In practice, however, protection relays typically require the excursion to persist for a specific duration (on the order of cycles) before triggering a trip. As a result, the certified safe reconnection time provides a margin relative to the actual relay tripping behavior, and incorporating a time delay coordination principle into the threshold analysis serves as a natural extension of this framework.

C. Earliest Reconnection Time

Let $x^-(t)$ denote the waiting trajectory generated by (9) with the DCL disconnected. Due to oscillatory swing dynamics, $x^-(t)$ may enter and exit a candidate safe set multiple times. However, for operational robustness, we require the reconnection time decision to satisfy a monotone safety property: if reconnection is certified safe at time t_1, it must remain certified safe for all $t > t_1$.

To formalize this requirement, we introduce the concept of a *certified safe reconnection set* $\mathcal{S}_{\text{safe}} \subseteq \mathcal{S}_{\text{adm}}$, which will be constructed in Section IV using energy function analysis.

In this hybrid framework, the system can be represented as a hybrid automaton with two discrete modes. *Mode 1* (DCL-disconnected): the state $x(t)$ evolves under (9) with guard condition $x^-(t) \notin \mathcal{S}_{\text{safe}}$. *Mode 2* (DCL-connected): the state evolves under (12) with guard condition $x^-(t_{\text{re}}) \in \mathcal{S}_{\text{safe}}$. The reset map at the switching instant $t = t_{\text{re}}^\star$ is the identity, since reconnection does not introduce a state jump. Fig. 2 illustrates the phase plane (δ, ω). During the waiting interval, the state evolves according to (9). Reconnection is permitted only when the trajectory reaches a switching state that is certified safe for post-reconnection dynamics and sufficiently settled under the dissipating pre-reconnection energy $E_{\text{pre}}(t)$.

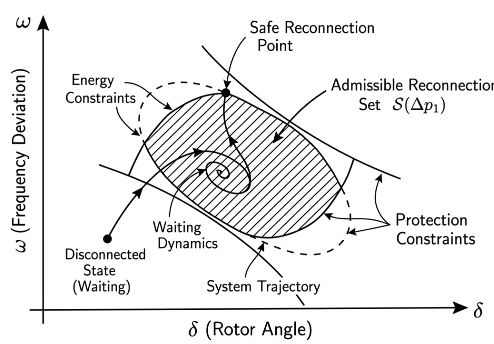

Fig. 2. Geometric interpretation in the (δ, ω) plane: the waiting trajectory $x^-(t)$ evolves under (9) until it enters the certified safe reconnection set $\mathcal{S}_{\text{safe}}$.

IV. Safe Reconnection Certification via Energy Function

Based on the dynamic model established in Section II, this section develops an energy-based certification framework for the safe reconnection of a DCL. A reconnection is certified as safe if it satisfies three conditions: (i) the state at the reconnection instant lies within admissible protection limits, (ii) the system settles into a state that is within the post-reconnection region of attraction, and (iii) the post-reconnection trajectory converges to the stable equilibrium of the load-connected system. To address the topological change induced by reconnection, we employ dual-energy functions for the pre- and post-reconnection phases [16].

A. Pre-Reconnection Energy Function

During the waiting interval $0 < t < t_{\text{re}}$, the DCL is disconnected and the generator dynamics follows the no-load swing equation (9). Let $\delta_{\text{eq}}^{\text{no-load}}$ denote the corresponding stable equilibrium satisfying $p_e^{\text{no-load}}(\delta_{\text{eq}}^{\text{no-load}}) = p_g$. The pre-reconnection energy function is defined as

$$E_{\text{pre}}(\delta, \omega) = \frac{1}{2} M \omega^2 + \underbrace{\int_{\delta_{\text{eq}}^{\text{no-load}}}^{\delta} \left[\frac{e}{x_d' + x_l^{\text{post}}} \sin\theta - p_g \right] d\delta}_{\Phi_{\text{pre}}(\delta)}. \tag{16}$$

Along the trajectories of the no-load dynamics, the time derivative satisfies $\dot{E}_{\text{pre}} = -D\omega^2 \le 0$, which means that all sublevel sets $\Omega_{\text{pre}}(c) := \{(\delta, \omega) : E_{\text{pre}} \le c\}$ are a forward invariant set.

Proof. By the chain rule and system dynamics (9),

$$\frac{d}{dt} E_{\text{pre}} = M\omega\dot{\omega} + \frac{\partial \Phi_{\text{pre}}}{\partial \delta} \dot{\delta} = M\omega\dot{\omega} + [p_e^{\text{no-load}}(\delta) - p_g]\omega$$

$$= \omega[p_g - p_e^{\text{no-load}}(\delta) - D\omega] + [p_e^{\text{no-load}}(\delta) - p_g]\omega$$
$$= -D\omega^2.$$

Since $D \geq 0$, we have $\dot{E}_{\text{pre}} \leq 0$. Forward invariance of sublevel sets $\{E_{\text{pre}} \leq c\}$ follows immediately from the non-increasing property. □

Let the pre-reconnection protection admissible region be

$$\mathcal{B} := \Big\{(\delta, \omega) \in \mathbb{R}^2 : \delta_{\min} \leq \delta \leq \delta_{\max},\ \omega_{\min} \leq \omega \leq \omega_{\max}\Big\}. \tag{17}$$

Denote the pre-reconnection vector field via

$$f_{\text{pre}}(\delta, \omega) = \begin{bmatrix} \omega \\ \frac{1}{M}\big(p_g - p_e^{\text{no-load}}(\delta) - D\omega\big) \end{bmatrix}. \tag{18}$$

We define the outward-pointing portion of the boundary as

$$\partial\mathcal{B}_{\text{out}} := \big\{x \in \partial\mathcal{B} :\ n(x)^\top f_{\text{pre}}(x) > 0\big\}, \tag{19}$$

where $n(x)$ is the outward unit normal to $\partial\mathcal{B}$.

Because E_{pre} is non-increasing, a trajectory starting from $x_0 := (\delta_0, \omega_0)$ can only reach states whose energy is less than or equal to $E_{\text{pre}}(x_0)$. Therefore, a sufficient no-escape condition is that the initial energy lies strictly below the minimum energy of all outward-pointing exit points as

$$E_{\text{pre}}(x_0) < \inf_{x \in \partial\mathcal{B}_{\text{out}}} E_{\text{pre}}(x). \tag{20}$$

This motivates the following robust critical-energy optimization as

$$E_{\text{crit,pre}} := \inf_{x \in \partial\mathcal{B}_{\text{out}}} E_{\text{pre}}(x). \tag{21}$$

Let $\partial\mathcal{B}_{\text{out}}$ be decomposed into four disjoint subsets corresponding to the faces of $\mathcal{B}$. For each face, the energy barrier is the infimum of E_{pre} over the outward-pointing region, which is defined as follows

$$E_{\delta^+} := \inf_{(\delta_{\max}, \omega) \in \partial\mathcal{B}_{\text{out}}} \Big\{E_{\text{pre}}(\delta_{\max}, \omega) : \omega > 0\Big\}, \tag{22a}$$

$$E_{\delta^-} := \inf_{(\delta_{\min}, \omega) \in \partial\mathcal{B}_{\text{out}}} \Big\{E_{\text{pre}}(\delta_{\min}, \omega) : \omega < 0\Big\}, \tag{22b}$$

$$E_{\omega^+} := \inf_{(\delta, \omega_{\max}) \in \partial\mathcal{B}_{\text{out}}} \Big\{E_{\text{pre}}(\delta, \omega_{\max})\ :\ \dot{\omega}(\delta, \omega_{\max}) > 0\Big\}, \tag{22c}$$

$$E_{\omega^-} := \inf_{(\delta, \omega_{\min}) \in \partial\mathcal{B}_{\text{out}}} \Big\{E_{\text{pre}}(\delta, \omega_{\min})\ :\ \dot{\omega}(\delta, \omega_{\min}) < 0\Big\}. \tag{22d}$$

The minimum barrier over all four faces defines the pre-reconnection critical energy as

$$E_{\text{crit,pre}} = \min\{E_{\delta^+}, E_{\delta^-}, E_{\omega^+}, E_{\omega^-}\}. \tag{23}$$

Therefore, the certified pre-reconnection safe set is the energy sublevel set

$$\mathcal{S}_{\text{pre}} := \big\{(\delta, \omega) \in \mathbb{R}^2 : E_{\text{pre}}(\delta, \omega) \leq E_{\text{crit,pre}}\big\}. \tag{24}$$

By construction, any trajectory originating in $\mathcal{S}_{\text{pre}}$ satisfies $E_{\text{pre}}(x(t)) \leq E_{\text{pre}}(x_0) \leq E_{\text{crit,pre}}$ for all $t \geq 0$. Consequently, it cannot reach $\partial\mathcal{B}_{\text{out}}$, as every point on $\partial\mathcal{B}_{\text{out}}$ has energy at least $E_{\text{crit,pre}}$.

B. Post-Reconnection Energy Function

At $t = t_{\text{re}}$, the DCL is reconnected and the dynamics switches to the load-connected system with a new equilibrium $\delta_{\text{eq}}^{\text{load}}$. The post-reconnection energy function $E_{\text{post}}(\delta, \omega)$ characterizes the ability of the system to absorb the transient induced by the load step as

$$E_{\text{post}}(\delta, \omega) = \frac{1}{2}M\omega^2 + \int_{\delta_{\text{eq}}^{\text{load}}}^{\delta} \Big[\underbrace{\frac{e\, v^{\text{post}}(\delta)}{x_d'} \sin\!\big(\theta - \varphi^{\text{post}}(\delta)\big)}_{p_e^{\text{load}}(\theta)} - p_g\Big]\, d\theta. \tag{25}$$

Along the trajectories of the post-reconnection dynamics, the time derivative satisfies $\dot{E}_{\text{post}} = -D\omega^2 \leq 0$, which ensures that the sublevel sets $\{E_{\text{post}} \leq c\}$ are forward invariant under the post-reconnection dynamics.

To determine the post-reconnection critical energy $E_{\text{crit,post}}$, a boundary sampling approach is employed. The critical energy is defined as the minimum post-reconnection energy over the sampled admissible boundary points associated with escape from the admissible operating region

$$E_{\text{crit,post}} := \inf_{x \in \partial\mathcal{S}_{\text{adm}}^{\text{out}}} E_{\text{post}}(x), \tag{26}$$

where $\partial\mathcal{S}_{\text{adm}}^{\text{out}}$ denotes the outward-pointing portion of the admissible boundary. This boundary includes points where either the rotor angle deviation reaches its limit, the frequency deviation reaches its limit, or the post-reconnection voltage constraint becomes active.

The $E_{\text{crit,post}}$ is computed by dense sampling of the admissible boundary and evaluating E_{post} at each feasible sampled point, which takes the minimum over all candidate boundary points. This yields an estimate of the post-reconnection critical energy that accounts for the nonlinear voltage-angle coupling.

For the damped swing model, the post-reconnection stability region can be characterized by the following energy-based safe set as

$$\mathcal{S}_{\text{post}} := \{(\delta, \omega) : E_{\text{post}}(\delta, \omega) < E_{\text{crit,post}}\}. \tag{27}$$

Any reconnection from a state $(\delta, \Delta\omega) \in \mathcal{S}_{\text{post}}$ is thereby certified to remain within the admissible operating boundary and converge to the stable equilibrium $(\delta_{\text{eq}}^{\text{load}}, 0)$ under the adopted energy-based boundary criterion.

C. Certified Safe Reconnection Set

In addition to the energy-based constraints $\mathcal{S}_{\text{pre}}$ and $\mathcal{S}_{\text{post}}$, reconnection must satisfy operational protection limits. The admissible set defined in (15) enforces the rotor-angle deviation bounds, the frequency deviation bounds and post-reconnection voltage limits. Thus, the certified safe reconnection region is characterized as the intersection of all three constraint sets as

$$\mathcal{S}_{\text{safe}} := \mathcal{S}_{\text{pre}} \cap \mathcal{S}_{\text{post}} \cap \mathcal{S}_{\text{adm}}. \tag{28}$$

The safe set $\mathcal{S}_{\text{safe}}$ is constructed by discrete sampling of the state space (δ, ω) over the operating region, which verify the three conditions in (24), (27) and (15) at the grid point.

Therefore, the earliest safe certified reconnection time is then defined as

$$t_{\mathrm{re}}^{*} = \inf\{\, t \geq 0 \mid x^{-}(t) \in \mathcal{S}_{\mathrm{safe}} \,\}. \tag{29}$$

Equivalently, this can be written as the solution of the optimization problem as

$$t_{\mathrm{re}}^{*} = \min_{t\geq 0} t \quad \text{subject to} \quad x^{-}(t) \in \mathcal{S}_{\mathrm{safe}}. \tag{30}$$

Because $\dot{E}_{\mathrm{pre}} \leq 0$, once the trajectory enters $\mathcal{S}_{\mathrm{pre}}$, it remains in $\mathcal{S}_{\mathrm{pre}}$ for all future time. This forward invariance, together with the post-reconnection energy certificate and admissibility constraints, ensures that reconnection at t_{re}^{*} leads to convergence without violating the operational limits.

V. Numerical Study

The proposed methodology was validated through numerical simulations on a single-machine infinite-bus (SMIB) system with a large-scale DCL, implemented in Julia. The system configuration follows the three-bus model described in Section II, with parameters chosen to represent realistic operating conditions for a medium-sized generator supplying a major data center facility as shown in Table I. The swing equation coefficient $M = 0.0146\,\mathrm{s}^2$ corresponds, for a 60 Hz system, to an inertia constant $H = M\omega_s/2 \approx 2.75\,\mathrm{s}$. This value lies near the lower end of the typical range for synchronous generators ($H \approx 1.75$–$10\,\mathrm{s}$ [19]), and is therefore representative of a small generating unit or a low-inertia operating condition. Such conditions are consistent with systems experiencing high converter-interfaced generation penetration, where reduced synchronous inertia can make the reconnection timing decisions more critical.

The numerical results were generated by discrete sampling of the state of the system. The critical energies $E_{\mathrm{crit,pre}}$ and $E_{\mathrm{crit,post}}$ are computed by boundary optimization and sampling, respectively. A 140×140 uniform grid over the protection region classifies states based on three criteria: pre-reconnection energy $E_{\mathrm{pre}} \leq E_{\mathrm{crit,pre}}$, post-reconnection energy $E_{\mathrm{post}} < E_{\mathrm{crit,post}}$, and admissibility constraints, which characterizes the safe reconnection region $\mathcal{S}_{\mathrm{safe}}$. Trajectory sampling with $\Delta t = 1$ ms resolution along post-fault dynamics identifies the optimal reconnection time $t_{\mathrm{re}}^{\star}$ as the first state entering $\mathcal{S}_{\mathrm{safe}}$.

A. System Equilibrium Points

The system equilibria were computed for three operating conditions: pre-fault, no-load (DCL disconnected), and post-fault with DCL reconnected. The results are presented in Table II. The critical energies are computed as $E_{\mathrm{crit,pre}}$ is equal to 0.0299 p.u. and $E_{\mathrm{crit,post}}$ is equal to 0.0331 p.u.. The pre-reconnection critical energy is dominated by the right boundary, which indicates that escape toward higher rotor angles is the limiting pre-reconnection mechanism. The slight difference between $E_{\mathrm{crit,pre}}$ and $E_{\mathrm{crit,post}}$ arises from the post-reconnection load connected dynamics, which may be attributed to the voltage-angle coupling.

Fig. 3 shows the phase portrait with the safe reconnection set $\mathcal{S}_{\mathrm{safe}}$ (green region), which represents the intersection of $\mathcal{S}_{\mathrm{pre}}$ (light blue), $\mathcal{S}_{\mathrm{post}}$ (orange), and $\mathcal{S}_{\mathrm{adm}}$ (light gray). The safe set occupies approximately 10.5% of the admissible region. The waiting trajectory (black line) and post-reconnection trajectory (red line) are shown, with optimal reconnection occurring at $t_{\mathrm{re}}^{\star} = 0.487$ s (marked by star).

Fig. 4 illustrates the frequency deviation during the post-reconnection phase for the safe scenario. After reconnection at $t_{\mathrm{re}}^{\star} = 0.487$ s, the system exhibits damped oscillatory response with initial deviation $\Delta\omega = -1.40$ rad/s, which converge to equilibrium within approximately 5 seconds. The response remains within protection limits (± 2.0 rad/s) throughout, demonstrating stable recovery. To validate the importance of proper reconnection timing, we simulated an unsafe reconnection scenario at $t_{\mathrm{re}} = 0.300$ s. As shown

TABLE I
System Parameters

Parameter	Symbol	Value	Unit
Generator Parameters			
Inertia constant	M	0.0146	s^2
Damping coefficient	D	0.05	p.u.
Internal voltage	e	1.05	p.u.
Transient reactance	x_d'	0.3	p.u.
Mechanical power	P_g	0.8	p.u.
Network Parameters			
Pre-fault line reactance	x_l^{pre}	0.4	p.u.
Fault-on reactance	x_l^{f}	5.0	p.u.
Post-fault line reactance	x_l^{post}	0.5	p.u.
DCL Parameters			
Active power	P_{DCL}	0.5	p.u.
Reactive power	Q_{DCL}	0.2	p.u.
Protection Limits			
Maximum angle deviation	$\delta_{\max}$	± 30	degrees
Maximum frequency deviation	$\omega_{\max}$	± 2.0	rad/s
Voltage limits	$V_{\min}, V_{\max}$	0.9, 1.1	p.u.
Synchronous frequency	ω_s	$2\pi \times 60$	rad/s

TABLE II
System Equilibrium Points

Operating Condition	Rotor Angle δ (deg)	V. Angle ϕ (deg)	V. Mag. V (p.u.)	Electr. Power P_e (p.u.)
Pre-fault	20.66	7.08	0.9733	0.800
No-load	37.56	—	≈ 1.00	0.800
Post-fault	21.78	9.16	1.046	0.800

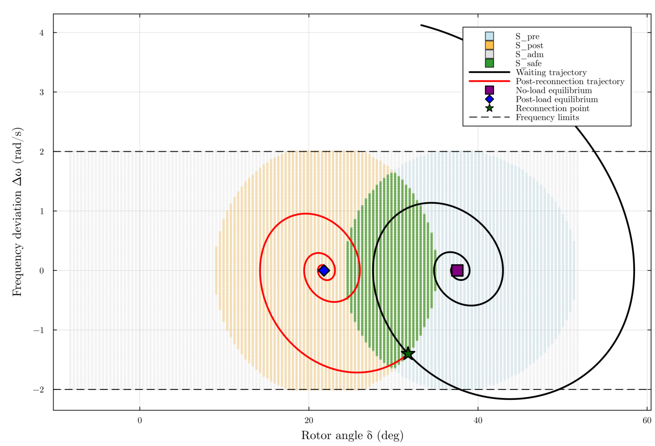

Fig. 3. Phase portrait showing safe set $\mathcal{S}_{\mathrm{safe}}$ and system trajectories.

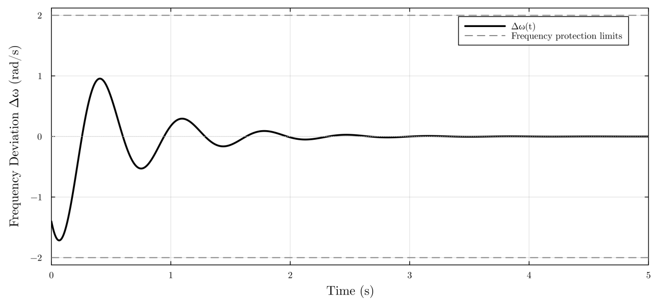

Fig. 4. Frequency deviation following safe reconnection at $t^{\star}_{\mathrm{re}} = 0.487$ s.

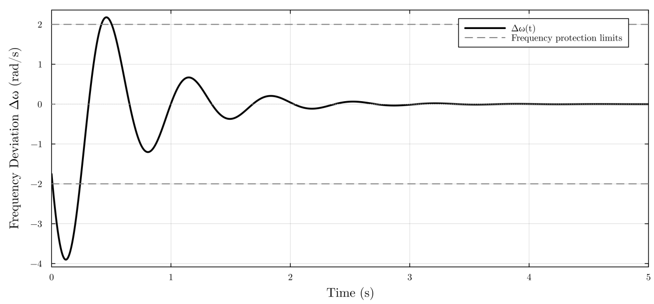

Fig. 5. Frequency deviation following unsafe reconnection at $t_{\mathrm{re}} = 0.3$ s.

in Fig. 5, early reconnection leads to oscillations exceeding protection limits, reaching approximately -3.5 rad/s, demonstrating system instability.

VI. Conclusion

This paper develops an energy-based analytical framework for determining safe reconnection time for large-scale DCL following grid disturbances. The approach addresses a critical gap in operational decision-making by providing a computationally efficient screening criterion that can inform reconnection policies and coordination between data center UPS controls and system operators. The proposed approach is effective in preventing flapping while ensuring post-reconnection stability.

The key contributions are: (i) a dual energy function methodology that enforces stability conditions both before and after reconnection, which accounts for the voltage-angle coupling introduced by constant power DCL, and (ii) a robust boundary optimization formulation for computing critical energy values that define the safe sets.

The validation results demonstrate that the proposed dual-energy-function framework accurately identifies a certified safe reconnection time that guarantees stable post-reconnection behavior. The method successfully distinguishes between safe and unsafe reconnection scenarios without requiring time domain simulations.

Future work will focus on: (i) extending the framework to multi-machine systems and multiple DCLs reconnecting at different times; (ii) validating the method on IEEE benchmark test systems to assess applicability beyond the three-bus model; and (iii) incorporating explicit AVR, Power System Stabilizer (PSS), and governor dynamics to quantify the conservatism of the constant-emf assumption and refine the voltage bounds in the safe set construction.

VII. AI Usage Disclosure

ChatGPT has been used for spell- and grammar-checking, and style improvements.

References

[1] International Energy Agency, "Electricity 2024: Analysis and forecast to 2026," report, International Energy Agency, Jan. 2024.

[2] International Energy Agency, "Energy and AI," report, International Energy Agency, Apr. 2025.

[3] S. Saha, M. I. Saleem, and T. K. Roy, "Impact of high penetration of renewable energy sources on grid frequency behaviour," *Int. J. Electr. Power Energy Syst.*, vol. 145, pp. 1–13, Feb. 2023. Art. no. 108701.

[4] B. Elenga Baningobera, I. Oleinikova, and K. Uhlen, "Optimizing frequency stability with adaptive fast frequency reserves and Wide-Area Monitoring Systems," *Int. J. Electr. Power Energy Syst.*, vol. 171, Oct. 2025. Art. no. 110951.

[5] J. M. Guerrero, L. G. de Vicuña, and J. Uceda, "Uninterruptible power supply systems provide protection," *IEEE Ind. Electron. Mag.*, vol. 1, pp. 28–38, Mar. 2007.

[6] J. M. Guerrero, L. Hang, and J. Uceda, "Control of distributed uninterruptible power supply systems," *IEEE Trans. Ind. Electron.*, vol. 55, pp. 2845–2859, Aug. 2008.

[7] "IEC 62040-3:2021: Uninterruptible power systems (UPS) – part 3: Method of specifying the performance and test requirements," Apr. 2021.

[8] "IEEE Std 1159-2019: Recommended practice for monitoring electric power quality," Aug. 2019.

[9] P. S. Kundur, *Power System Stability and Control*. New York, NY, USA: McGraw-Hill, 1994.

[10] A. Jiménez-Ruiz and F. Milano, "Data center model for transient stability analysis of power systems." arXiv:2505.16575, May 2025.

[11] T. Kërçi, C. Duggan, U. Farooq, S. Tweed, and M. Val Escudero, "Impact of converter-based demand on frequency quality in the Ireland and Northern Ireland power systems," in *Proc. CIGRE Paris Session*, no. C4-10907-2024, 2024.

[12] Commission for Regulation of Utilities, "Direction to the system operators related to data centre grid connection processing," Decision Paper CRU/21/124, Commission for Regulation of Utilities, Dublin, Ireland, Nov. 2021.

[13] L. R. Gorjão, L. Vanfretti, D. Witthaut, C. Beck, and B. Schäfer, "Phase and amplitude synchronization in power-grid frequency fluctuations in the Nordic grid," *IEEE Access*, vol. 10, pp. 18065–18073, 2022.

[14] M. A. Pai, *Energy Function Analysis for Power System Stability*. New York, NY, USA: Springer, 1989.

[15] W. W. Price, C. W. Taylor, and G. J. Rogers, "Standard load models for power flow and dynamic performance simulation," *IEEE Trans. Power Syst.*, vol. 10, pp. 1302–1313, Aug. 1995.

[16] P. W. Sauer, M. A. Pai, and J. H. Chow, *Power System Dynamics and Stability: With Synchrophasor Measurement and Power System Toolbox*. Wiley-IEEE Press, 2 ed., 2017.

[17] "PRC-024-3: Frequency and voltage protection settings for generating resources," July 2020. Effective: Oct. 1, 2022.

[18] "IEEE Guide for Abnormal Frequency Protection for Power Generating Plants," 2018. Reaffirmed 2018.

[19] B. Tan, J. Zhao, M. Netto, V. Krishnan, V. Terzija, and Y. Zhang, "Power system inertia estimation: Review of methods and the impacts of converter-interfaced generations," *Int. J. Electr. Power Energy Syst.*, vol. 134, 2022. Art. no. 107362.

I. Review #225A

A. Paper summary

The paper proposes a method for assessing safe reconnection times for data centre loads to avoid transient dynamic issues in the system. A simplified model is developed and an analytical assessment framework is proposed. This is then confirmed to be appropriate using numerical simulation of the same test system. This is interesting work, but could be more comprehensively verified and validated against models with more complex models to assess if the simplifications made have significant impacts on how much the results can be generalised.

B. Comments for authors

The following aspects should be considered in order to improve the paper:

1) The introductory statement about the worldwide level of data centre load shows it is significant, but the problem will probably appear more acute if you highlight specific concentrations of data centre load. You mention the Irish system conditions later, I would suggest bringing this forward and emphasising the statistics you have.
2) In the introduction and justification for the work, aspects related to voltage magnitude management are mentioned (as a potential cause of issues, for example with voltage threshold violations causing flapping). However the model assumes constant generator emf (for analytical simplicity). How much of a challenge is it to include some kind of generator AVR? Under what kind of conditions (what type of AVR, reactive power capability etc) would your model (with constant excitation) be valid and when might it start to fail? The statement ”For simplicity, we assume that the voltage magnitude at bus 1, the back emf of the synchronous generator, is constant, even during transients.” is doing a lot of heavy lifting and I think you need to do a little more to verify that this is appropriate for your specific study (even if it is commonly assumed for other equal area criteria-type analysis). I assume that Section III.B.2 on voltage bounds would be affected quite significantly by more explicit consideration of AVRs and Vac or reactive power support from other devices. At the very least, I'd like to see some explicit discussion of how this would vary in formulation when the present simplifications about voltages are removed.
3) Similarly to the above comment - I really believe that you need to verify your results against a more complex model. You have created the simplified representation to perform the analysis, and then ”validated” against the same simplified extended SMIB in the time domain. Whilst this shows that the analytical approach is correctly assessing the stability margins for your selected model, it does not show that this approach is valid for assessing the actual safe reconnection times for large scale data centre loads when you take the more detailed dynamic behaviour into account. There are, clearly, many aspects which have been omitted from the model - even if it were to remain at the same scale (3 bus). The controls acting on the same timescale of interest as this dynamic study should be re-introduced in order to assess the validity of the proposed method. The most critical aspects to include would be any voltage or frequency regulation controls or dynamic voltage or frequency containment services (from generators or other devices - say batteries).
4) The mathematical derivation is presented clearly and consistently and provides useful information about reproducibility should any readers of the paper wish to implement the same method. No change required. This is a positive of the paper.

- Minor, but I would avoid the use of DC as an acronym for data centre considering DC has a much longer-established acronym usage in the power systems space. Phrases like ”DC load” can be confusing when first read. If it is most commonly used as DC load, then maybe use DCL to avoid confusion, if you need an acronym. Saying data centre load is also fine.
- Make sure that all your figures are well proportioned and well designed. Some fonts and text should be a little larger (for example in legends) to be more readable. Some dashed lines (like in Fig 4) are a little hard to distinguish so it would be good to consider making this more legible. On page 6, you have some paragraph spacing, whereas the rest of the paper does not.

C. Summarize your recommendation in one to two sentences

The paper is clear, and well laid out, but would benefit from more thorough verification against time-domain models which do not include the same simplifications - particularly surrounding voltage controllers. Ideally, you could also include these considerations around voltage behaviour directly into the method.

— *Robin Preece*

II. Review #225B

A. Paper summary

The paper studies the problem of safely reconnecting large data center (DC) loads after a disturbance to avoid repeated connect–disconnect behavior (flapping). The authors develop an analytical framework based on a simplified three-bus system and use energy-function and Lyapunov methods to determine the earliest safe reconnection time that guarantees convergence to a stable equilibrium and prevents protection limit violations.

B. *Comments for authors*

The paper proposes a formal framework to avoid flapping during disturbances in power networks hosting large data center loads. The topic is timely and relevant, and the analytical approach based on Lyapunov methods and energy functions is interesting. My main comments are listed below.

1) Hybrid system representation. In the list of contributions, the authors mention a hybrid system representation of the DC disconnection/reconnection dynamics. However, while switching between dynamics is described (e.g., pre-reconnection and post-reconnection models), I could not find a formal hybrid system representation (e.g., explicit definition of modes, switching conditions, and guard sets). Clarifying this point would help make the modeling contribution more precise.
2) Conditions leading to flapping. The paper states that the proposed method guarantees that flapping will not occur if reconnection happens after the computed safe time. It would be helpful if the authors explicitly described the conditions under which flapping occurs in the model. In particular, does flapping arise when the system evolves under the post-reconnection dynamics in (12) while violating the protection limits?
3) Fixed-point iteration and network parameters. Please clarify how the line reactance x_l changes during the fault event and how this affects the algebraic equations used to compute the voltage. Additionally, the steady-state voltage is obtained through the fixed-point iteration in (4). Is convergence of this iteration always guaranteed? If not, under what conditions does it converge?
4) Extension to multiple data centers. The framework is developed for a single DC connected to a simplified three-bus system. How difficult would it be to extend the approach to the case of multiple DC loads reconnecting at different times?
5) Numerical validation. The numerical validation is performed on a simplified three-bus system. Additional simulations on more representative network models (e.g., IEEE benchmark test systems) would help demonstrate whether the proposed method, even though derived on a simplified model, can be applied to more realistic power networks.

C. *Summarize your recommendation in one to two sentences*

The paper addresses a timely problem related to the integration of large data centers in power systems. The proposed method provides analytical guarantees that flapping will not occur in the simplified model considered; however, additional validation on more realistic power-system test cases (e.g., IEEE benchmark systems) would help assess the practical applicability of the approach.

— *Guido Cavraro*

III. Review #225C

A. *Paper summary*

The paper presents an energy based approach for identifying the safe reconnection time of Data Centres following a disconnection. The method is tested on a modified SMIB system and an analytical derivation is calculated which then leads to an optimisation problem formulation to ensure state variables remain bound within safe trajectories that will not trigger protection devices.

B. *Comments for authors*

The paper is well written and presented and the analytical derivation is very useful in providing a safe reconnection time criterion. The subject is interesting and addresses an emerging issue. Some detailed points follow:

1) The first contribution of the paper (the development of an extended SMIB system) is a bit overstated I believe. It effectively consists of adding an additional bus where the dc load is disconnected, however this appears to be treated as just a simple load with constant power demand.
2) While expected with analytical methods and the motivation for this is certainly justified, there are several simplifications which I believe need to discussed along with any potential implications (maybe in a short discussion section?):
   a) The synchronous machine assumes constant field and no AVR/PSS. This is expected to affect the trajectory of voltage/angle. How much could this affect the analysis?
   b) The fault is assumed to be immediately cleared and consequently the fault-on trajectory that would cause the dc load to trip in the first instance is neglected. What are the implications of this?
   c) The synchronous machine is assumed to feed only the dc load and is unloaded when the dc load is disconnected. Is this is a very particular case or can be generalised for the more standard case where the machine will be providing power to the infinite bus too.
   d) The load of the data-centre is considered to be constant PQ load as I understand it. In reality, data centres I believe can "cycle" changing load quite quickly. While I understand this might not be entirely relevant with the particular case studied, I am wondering whether the original motivation of the paper with respect to "flapping" might also be affected by this behaviour too? – a brief discussion might be useful.

3) The method appears to be conservative in the sense that any instantaneous violation of the set protection thresholds is assumed to cause a disconnection and consequently has to be avoided. In reality, typically there are time delays so the violation needs to be sustained for a given amount of time to cause a trip. Has this been considered? Some discussion around how conservative the method is would be useful. For example in fig. 5, would the duration of this violation cause a protection device to trip?
4) Linking a bit with the previous comment, the inertia constant of the tested system appears to be (unrealistically) small (0.0146 seconds). Could you please comment on this choice? This links to results shown in fig. 5 also where the frequency appears to have very large swings.
5) The validation is sound, however a more interesting validation would entail a more detailed time domain model that captures detailed dynamics (e.g. 6th order) of synchronous machines, including AVR/PSS/Governor. This would allow quantifying things like how conservative the method is. Even more so what happens with converters present would also be very interesting but I understand this last part might fall outside of the scope of the paper.

C. Summarize your recommendation in one to two sentences

Overall a well written paper with very interesting analysis that introduces a way to define the reconnection time of data centres ensuring no protection limit violations happen. Additional discussion on limitations and how conservative the approach might be would be welcome.

— *Panagiotis Papadopoulos*

IV. Brief response to reviewers (optional)

We thank the reviewers for their careful reading and constructive comments. The final version has been revised to address the main points raised while avoiding major changes to the paper's content.

In response to comments from Reviewers 225A and 225C on modeling assumptions, we added a discussion of the constant-emf synchronous-machine representation in Section II-A. The revised text clarifies that this assumption is consistent with classical first-swing transient-stability analysis, identifies the operating conditions under which it is most appropriate, and explains that explicit Automatic Voltage Regulator (AVR) dynamics would primarily affect the post-reconnection voltage bounds in the safe set construction, and that quantifying this effect is outside the scope of the present work. Extension to include AVR, Power System Stabilizer (PSS), and governor dynamics is identified as future work in the conclusion.

In response to comments from Reviewer 225B on the hybrid nature of the problem, we added a formal hybrid system description in Section III-C, which includes the DCL-disconnected and DCL-connected modes, the guard condition for reconnection, and the identity reset map. We also clarified that the present formulation treats instantaneous threshold violations as disconnection events, while practical protection devices may include time-delay characteristics. Incorporating such time-delay logic is identified as a future extension.

In response to comments from Reviewers 225B and 225C on the fixed-point calculation and inertia value, respectively, we added a remark clarifying the real-valued and local convergence conditions for the fixed-point iteration, and we revised Section V to relate the swing equation coefficient $M = 0.0146$ s^2 to the standard inertia constant $H \approx 2.75$ s supported by a cited review of power system inertia constants.

Finally, we improved figure readability, and expanded the conclusion to explicitly identify validation on IEEE benchmark systems, multi-DCL reconnection, and higher-order generator/control modeling as future research directions.

V. Brief summary of changes made to the final paper

The following changes were made to the final version of the paper.

The terminology was revised throughout the paper by replacing ambiguous uses of "DC load" with "data center load (DCL)" to avoid confusion with the conventional meaning of DC as direct current in power systems literature.

Section II-A was expanded to discuss the constant internal-emf assumption used in the reduced-order synchronous machine model. The added text explains that this assumption is standard in classical first-swing transient stability analysis and clarifies that explicit Automatic Voltage Regulator (AVR) dynamics would primarily affect the post-reconnection voltage bounds, and that quantifying this effect is outside the scope of the present work.

Section II-B was revised to add a remark clarifying that the fixed-point iteration is real-valued only when the arguments of the square root are nonnegative, while convergence is expected when the corresponding fixed-point map is locally contractive.

Section III-B was revised to clarify the flapping condition and the interpretation of protection thresholds. The revised text states that flapping occurs when the post-reconnection trajectory violates the protection limits, thereby re-triggering the UPS disconnection condition. The paper also notes that real protection devices usually require threshold violations to persist for a finite time before tripping, while the proposed method models threshold crossing as an immediate disconnection event.

Section III-C was revised to include a formal hybrid system description of the DCL disconnection/reconnection process, which includes the DCL-disconnected and DCL-connected modes, the guard condition based on the certified safe reconnection set, and the identity reset map at reconnection.

Section V was revised to express the swing equation coefficient $M = 0.0146\ \mathrm{s}^2$ in terms of the standard inertia constant $H \approx 2.75$ s, and to explain that this value represents a relatively low-inertia operating condition.

Finally, the conclusion was expanded to identify future work, which includes extension to multi-machine systems, multiple independently reconnecting DCLs, validation on IEEE benchmark systems, and incorporation of AVR, PSS, and governor dynamics. The readability of the figures was also improved by increasing the legend and font sizes.